

1 Hydrothermal conversion of different lignocellulosic biomass feedstocks – 2 Effect of the process conditions on hydrochar structures

3
4 Fatih Güleç^{1*}, Luis Miguel Garcia Riesco¹, Orla Williams¹, Emily T. Kostas², Abby Samson³,
5 Edward Lester¹

6
7 ¹*Advanced Materials Research Group, Faculty of Engineering, University of Nottingham, Nottingham,*
8 *NG7 2RD, UK*

9 ²*Advanced Centre of Biochemical Engineering, Bernard Katz Building, University College London,*
10 *Gower Street, London WC1H 6BT, UK*

11 ³*Department of Mechanical Engineering, University of Sheffield, Sheffield, S3 7RD, UK*

12 **Fatih.Gulec1@nottingham.ac.uk, Gulec.Fatih@outlook.com*

13 14 **Abstract**

15 Five biomass feedstocks (Coffee residues, Rice waste, Whitewood, Zilkha black, and Lignin) were
16 hydrothermally processed in a semi-continuous flow rig using 9 different processing conditions (75,
17 150, 250 °C, and 1, 50, 240 bar). Solid residues produced at low temperature (<150 °C) did not show
18 significant structural changes. At more severe conditions, structural changes could be linked to the
19 lignocellulosic composition and divided into three categories: (i) biomass with higher hemicellulose-
20 cellulose and lower cellulose-lignin structures, (ii) lower hemicellulose-cellulose and higher cellulose-
21 lignin structures, and (iii) only cellulose-lignin structures. Both hemicellulose and cellulose structures
22 in category (i) and (ii) were successfully degraded under subcritical conditions (250 °C and 50 bar) to
23 produce hydrochar with higher lignin content. Biomasses with higher levels of lignin did not show the
24 same degree of transformation. Category (i) produced a low hydrochar yield (39 wt.%) due to the
25 degradation of higher hemicellulose-cellulose structures. Category (ii) had higher hydrochar yields (58-
26 62 wt.%) due to the lower amount of cellulose and hemicellulose. Category (iii) had the highest
27 hydrochar yields (73-90 wt.%) thanks to the lack of hemicellulose and lower cellulosic structures. A
28 novel concept called “displacement”, based on a thermogravimetric profiling method, was used to
29 quantify changes in the pyrolysis behaviour of the hydrochar compared to the original feedstock. The
30 degree of “displacement” correlated with hydrochar yield and reactivity, the highest level of
31 displacement was observed with category (i- higher hemicellulose-cellulose biomasses) while the lowest
32 displacement was observed with category (iii- higher lignin biomasses). This novel technique could be
33 used to quantify the effects of hydrothermal treatment on any given biomass.

34
35 **Keywords:** Hydrothermal conversion, Hydrochar, Bioenergy, Lignocellulosic Biomass, Displacement.

36 **1 Introduction**

37 Thermal and biological biomass processing technologies such as pyrolysis, combustion,
38 hydrothermal processes (liquefaction, gasification, and carbonisation) and biochemical
39 conversion have all been identified as pathways to decrease CO₂ emissions and reach the 2 °C
40 climate target [1]. Biomass is defined as inexpensive, clean, and environmentally friendly
41 energy sources [2, 3] and an integral part of the global carbon cycle [4]. However, there are
42 several obstacles to the full commercialisation of bioenergy and bioproducts via these
43 technologies, which include the resourcing of biomass, inadequate biomass refinery
44 technologies, a lack of cost-competitive bioproducts and a limited and/or unstable supply of
45 biofuels and bioproducts [5]. Furthermore, the chemical and biological variations in different
46 types of biomass can result in significant changes in characteristics (grinding, handling,
47 composition etc) that can hinder the commercialisation of these technologies[6-8].
48 Lignocellulosic biomass feedstocks are defined as one of the crucial renewable energy sources
49 thanks to its availability, high energy content, and reactivity. The lignocellulosic biomass chars
50 can be produced by pyrolysis, torrefaction, and hydrothermal processes [9]. The lignocellulosic
51 biomasses are composed of hemicellulose, cellulose, and lignin in addition to a small quantity
52 of extractives and ashes [10]. Although the composition of lignocellulosic biomass varies
53 according to the type, location, maturity, and climate conditions, on average it consists of about
54 15-30% of hemicellulose, 40-60% of cellulose, and 10-25% of lignin [11].

55

56 Hydrothermal processing is one of the most promising technologies, as it can use the high
57 inherent moisture of biomass to its advantage [12]. For other processing techniques, such as
58 pyrolysis and combustion, the high moisture content needs to be removed which requires a
59 significant amount of energy for drying processes. In contrast, hydrothermal conversion of
60 biomass in hot-compressed water is a viable, scalable, and energy-efficient thermo-chemical
61 route for converting biomass into a synthetic solid, liquid, or gaseous fuels and chemicals [13].
62 In hydrothermal treatments, water can be a solvent, a reactant and/or a catalyst in the hydrolysis
63 reactions. The process also leads to by-products that can be used for power generation and the
64 recovery of useful nutrients [14]. In this process, the biomass conversion is carried out by
65 several complex reactions depending on the physical properties of the water, which are usually
66 manipulated changing the temperature, pressure, and contact time of the water-biomass in order
67 to obtain the desired products. The hydrothermal conversion is therefore classified into three

68 processes namely carbonisation, liquefaction and gasification depending on the severity of the
69 operating conditions [15-18].

70

71 Hydrothermal gasification (HTG, >350 °C) is carried out near-critical or above-critical
72 conditions to produce a synthetic fuel gas (syngas), which is rich in CH₄, H₂, CO₂, and CO
73 depending on experimental conditions [15]. Depending on the biomass, the syngas may contain
74 a significant amount of undesirable impurities such as sulphur compounds (SO₂), nitrogen
75 compounds (NH₃ and HCN), hydrogen halides (HCl and HF) [16]. Hydrothermal liquefaction
76 (HTL, 250-370 °C, 50-240 bar) is the wet processing route for high moisture biomasses to
77 produce of a liquid fuel (bio-crude) [15], which is similar to petroleum crude and can be
78 upgraded to a range of petroleum-derived fuel products [17]. Since HTL involves the direct
79 conversion of the biomass into bio-crude in the presence of a solvent, it eliminates the high
80 drying costs [18-20]. Hydrothermal carbonization (HTC, 180-250 °C, 15-40 bar) is a
81 thermochemical process for the pre-treatment of high moisture content biomass to make it
82 viable in for energy production [17, 21, 22]. HTC uses relatively low temperatures and is
83 suitable for any kind of biomass feedstock [23]. HTC can convert lignocellulosic materials into
84 solid hydrochar, which have better physicochemical characteristics than raw biomass
85 feedstocks [24], and also produce liquid products that contain organic and inorganic value-
86 added chemicals [25]. The HTC hydrochars exhibits lower O/C and H/C ratios compared to dry
87 torrefaction and turn into more lignin or coal type materials [26]. HTC hydrochars can be used
88 in a wide range of processes such as soil amendment [27], CO₂ capture [28], nanoparticles (for
89 making composites) [29], energy production [30], water purification [31] thanks to their
90 physicochemical properties [32]. Although the lab-scale research on HTC of various biomass
91 feedstocks has been recently progressed and provided significantly promising results, the HTC
92 process needs further investigations in terms of process and reactor types, biomass feedstocks,
93 and conditions due to the complex reaction mechanisms and operational barriers to make this
94 technology as a commercial technology [25]. For example, a continuous HTC process would
95 be one of the key components for a potential industrial application of HTC, as most HTC
96 research have been carried out in batch [25].

97

98 In this study, the hydrothermal conversion of five different lignocellulosic biomass feedstocks
99 (Coffee residues, Whitewood, Rice waste, Zilkha black, and Lignin) was investigated in a semi-
100 continuous process at different temperatures (75, 150, and 250 °C) and pressures (1, 50 and 240

101 bar) to produce hydrochars. Each hydrochar sample was characterised in a Thermogravimetric
102 Analyser (TGA) using a slow pyrolysis methodology to identify the effects of hydrothermal
103 treatments on hydrochar structures using thermal decomposition behaviours. Additionally, a
104 new method called “displacement” was shown to provide quantitative information about the
105 impact of hydrothermal treatment on the lignocellulosic composition of biomass feedstocks.
106 This method has been previously used as a fingerprint technique for biomass identification as
107 it can quantify hemicellulose, cellulose and lignin levels present in any type of biomass [33].

108

109 **2 Material and Methods**

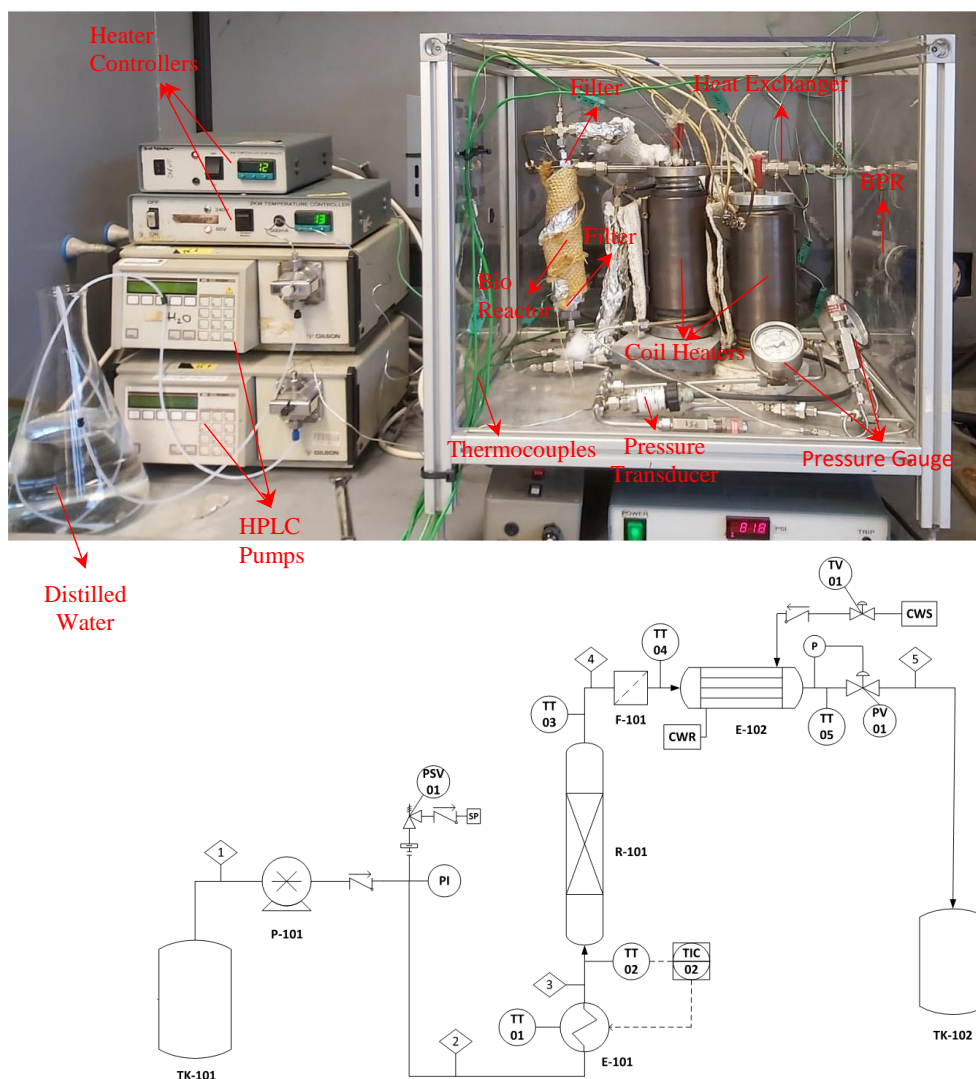
110 The effects of the hydrothermal conversion process conditions on the hydrochar structures were
111 investigated using five different biomass feedstocks namely Coffee residues (CR, as an
112 industrial waste, obtained from spent aluminum capsules used in certain domestic coffee
113 machines), Whitewood (WW, as a forest waste, obtained from sawdust of white wood), Rice
114 waste (RW, as a food waste, obtained from rice pellets), and Zilkha black (steam exploded
115 white wood pellets) and Lignin (ZB and LG as high carbon ratio materials, obtained from Zilkha
116 Black® pellets and Lignin pellets). These feedstocks have been selected due to their abundance
117 in environment and commercial availability, as well as their potential to produce hydrochars
118 having different properties [6, 34, 35]. Zilkha was chosen as it represents a wood based,
119 lignocellulosic feedstock but one that has already been pretreated/upgraded using thermal
120 methods. The biomass feedstocks (CR, WW, RW, ZB and LG) were firstly ground into a
121 powder and sieved in particle sizes of 200-1000 µm in a sieve shaker for 15 minutes using the
122 standard method of EN ISO 17827-2:2016 – *Solid biofuels – Determination of particle size
123 distribution for uncompressed fuels – Part 2: Vibrating screen method using sieves with
124 aperture of 3,15 mm and below* [36, 37].

125

126 **2.1. Hydrothermal processing**

127 The biomass feedstocks (CR, WW, RW, ZB, and LG) were hydrothermally processed using a
128 semi-continuous flow rig shown in Figure 1. The operation of the rig consists of a semi-
129 continuous reactor that works by preloading a biomass sample inside a 100 micron mesh and
130 processing using a semi-continuous hydrothermal flow. The feed stream (distilled water) TK-
131 101 is pumped using a high pressure Gilson HPLC pump (P-101) and preheated to the desired
132 temperature using a Watlow cartridge heater (E-101). The preheated water stream flows into
133 the reactor (R-101) from the bottom, where the reaction starts with the effects of matter and

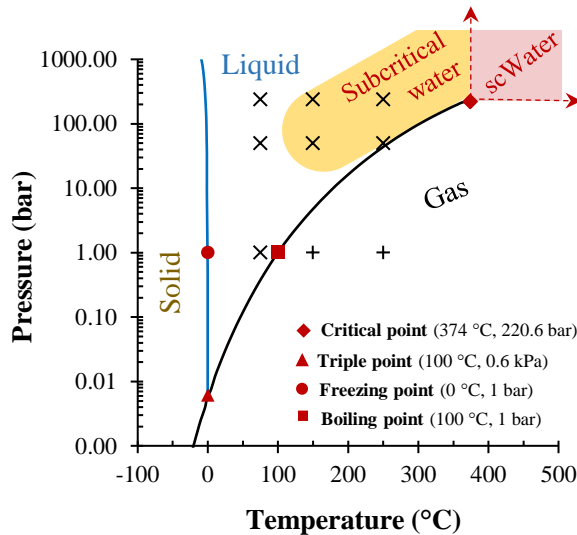
134 energy transfer. The enriched stream leaves the reactor and passes through a filter (F-101) of
 135 100 μm that retains any solids that could potentially have flowed out the top of the reactor.
 136 After the filter, the resulting products are cooled in a heat exchanger (E-102) with a stream of
 137 fresh water. Finally, the product stream goes through a back-pressure regulator (BPR) which
 138 pressurizes the whole system and the outflow is collected after the BPR (TK-102). The main
 139 focus of this study was the residual solids in the reactor rather than the contents of the liquid
 140 effluent.
 141



142
 143 **Figure 1.** Semi-continuous hydrothermal treatment process rig and flow diagram.
 144

145 The hydrothermal conversion of CR, WW, RW, ZB and LG were investigated at low to medium
 146 temperatures (75, 150, and 250 $^{\circ}\text{C}$) and pressures (1, 50, and 240 bar), as seen in
 147 Figure 2, to establish the optimal conditions for hydrochar production at low temperatures.

148 Approximately 5.0 g of each biomass feedstock (CR, WW, RW, ZB, and LG) was placed
 149 between two layers of sieves (100 µm) into the steel reactor. Once pressure had been obtained,
 150 the flow rates were reduced to a minimal level (1-5 ml/min) The hydrothermal rig was then
 151 pressurised using a distilled water flow rate of 20 ml/min. The heat exchanger temperature was
 152 then set the target temperature (75, 150, and 250 °C). Once the system had stabilised at the
 153 desired conditions, the water flow rates were then introduced to the reactor with a flow rate of
 154 20 ml/min. The total residence time of water in the reactor was determined about 1.9-2.3 min
 155 from pump to back pressure regulator. The liquid product stream was cooled to about 20-30 °C
 156 in a heat exchanger using a water stream and collected and then stored in a freezer at -18 °C for
 157 further analysis. The hydrochars were collected from the reactor and dried in an oven at 100 °C
 158 for overnight.
 159



160
 161 **Figure 2.** A schematic phase diagram showing Pressure – Temperature for water including
 162 the near and supercritical region (scWater). Plus (+) and Cross (x) signs represent the
 163 experiments investigated under vapour and liquid conditions, respectively.
 164

165 2.2. Char formation and analysis

166 The yield of hydrochar (or solid residue) after each hydrothermal conversion experiments
 167 was determined using the following equation (Eq-1) [38].

$$168 \text{ Solid residue (wt.\%)} = \frac{m_{char,dry}}{m_{biomass,dry}} * 100 \quad (1)$$

169 Where, $m_{char,dry}$: the dried weight of hydrochar (g) after hydrothermal conversion, $m_{char,dry}$:
 170 the dried weight of biomass (g) before hydrothermal conversion.

171 **2.3. Thermogravimetric Analysis**

172 A thermogravimetric characterisation technique was used to measure the pyrolysis and then
173 combustion behaviour of each biomass and hydrochar sample. This technique has been used
174 to quantify components such as hemicellulose, cellulose [33]. A TA-Q500 system was
175 loaded with approximately 15-25 mg of hydrochar (or raw biomass) using a platinum pan
176 4 mm deep and 10 mm in diameter. It was then heated from ambient temperature to 900 °C
177 with a heating rate of 5.0 °C/min under N₂ flow rate of 100 ml/min and held at this
178 temperature for about 5 minutes. N₂ was then replaced by air (to combust the fixed carbon)
179 with a flow rate of 100 ml/min at 900 °C for a further 10 minutes [33]. The devolatilization
180 behaviours of the biomass feedstocks and hydrochars were identified using the
181 thermogravimetric (TG) and differential thermogravimetric (dW/dt) curves [39]. The fuel
182 ratio was defined as the ratio of fixed carbon to volatile matter (dry ash free basis) for each
183 biomass and hydrochar. Based on this technique, we propose a new method called
184 “displacement” to characterize the impact of hydrothermal treatment. Displacement was
185 determined with the global sum of all absolute value of the differences between the original
186 and experimental DTG profiles as defined in Eq-2.

187
$$Displacement = \sum_{T=25^{\circ}C}^{T=900^{\circ}C} \left(\left| \left(\frac{dw}{dt} \right)_{bf,T} - \left(\frac{dw}{dt} \right)_{hc,T} \right| \right) \quad (2)$$

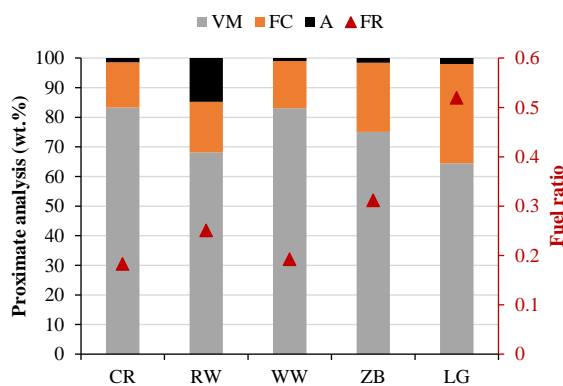
188 Where, T is the temperature of thermal decomposition (25-900 °C), $(dw/dt)_{bf,T}$ and
189 $(dw/dt)_{ch,T}$ are the weight loss rate of biomass feedstocks and hydrochars at the specific
190 temperatures in the thermal degradation process. Displacement is essentially a relative
191 measurement and can be applied to any biomass and resultant char. A large displacement
192 number means a large change in pyrolysis behaviour and this relates back to changes in
193 organic composition [33, 40]. These displacement calculations are based on the dW/dt
194 profiles shown in Figures 7,9,10,12 and 13. In essence, if the hydrochars profile is a close
195 match to the original biomass then values of 1000-2000 tend to result. If the profiles show
196 a marked difference in terms of in peak position (on the x-axis) or shape, then values of
197 5000-7000 tend to be seen.

198

199 **3 Results and Discussions**

200 **3.1. Characterisation of feedstocks**

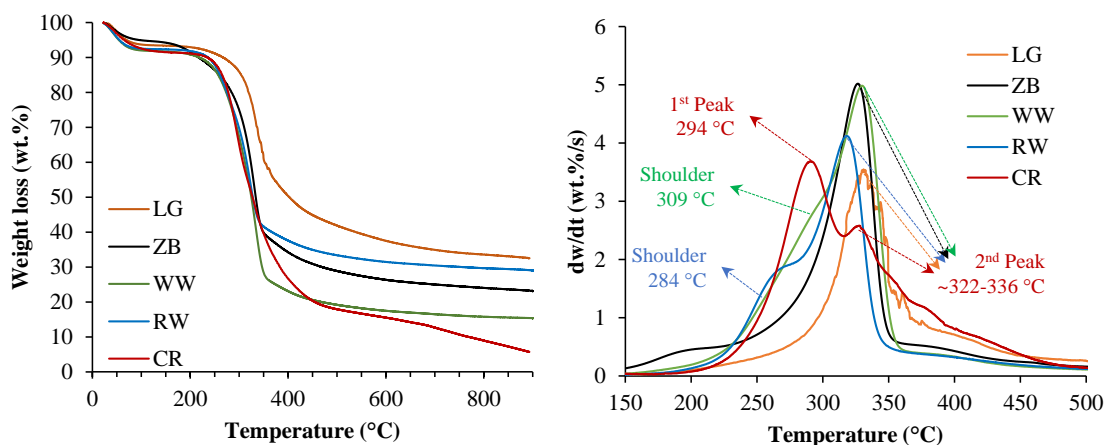
201 Proximate analysis of the lignocellulosic biomass feedstocks (LG, ZB, WW, RW, and CR) is
202 presented in Figure 3 and 4. Among these biomass feedstocks, the LG has the highest FC (~34
203 wt.%) and lowest volatile matter (~65 wt.%) ratios and ZB follow as second with the ~24 wt.%
204 of fixed carbon and ~75 wt.% of volatile matter. WW and CR demonstrate relatively similar
205 ratios ~15 wt.% of fixed carbon and ~83 wt.% of volatile matter with a low ash content (< ~2
206 wt.%). However, RW has a relatively high ash content (~15 wt.%) compared to the others.
207 Furthermore, LG has the highest fuel ratio (0.52), while CR and WW both have the lowest fuel
208 ratio at 0.19.



209

210 **Figure 3.** Proximate analysis (dry basis), fuel ratio (FR) of raw biomasses (CR-Coffee
211 residue, RW-Rice waste, WW-White wood, ZB- Zilkha black, LG-Lignin).

212



213

214 **Figure 4.** Weight loss and weight loss rates of the raw biomasses in slow pyrolysis (CR-
215 Coffee residue, RW-Rice waste, WW-White wood, ZB- Zilkha black, LG-Lignin).

216

217 The lignocellulosic biomass consists of lignin (15-35 %, non-carbohydrate source), cellulose

218 and hemicellulose (carbohydrate sources), and potentially lipids and proteins [41]. Therefore,
219 the thermal decomposition (slow pyrolysis) of the biomass feedstocks can provide detailed
220 information about the biomass structures such as hemicellulose (220-315 °C), cellulose (315-
221 400 °C), and lignin (160-900 °C) structures [33, 42, 43]. The DTG graph in Figure 4
222 demonstrates that LG and ZB provide only one strong peak at about ~330 °C, which
223 demonstrates the high cellulose-lignin content. Furthermore, CR is the only biomass which
224 demonstrates two clear peaks; the first one is at ~290 °C based on hemicellulose-cellulose
225 structure and the second one is at ~330 °C based on the cellulose-lignin structures. Additionally,
226 there is a strong tail after the second peak which indicates a high lignin content in CR. However,
227 WW and RW provide one peak at ~322 °C (which is the structure of cellulose-lignin) with a
228 detectable shoulder at 280-300 °C (originating from the hemicellulose-cellulose structures of
229 WW and RW).

230

231 **3.2. Solid residue-Hydrochar formation**

232 After the hydrothermal conversion of biomass feedstocks (CR, WW, RW, ZB, and LG), the
233 solid residue (or hydrochar) yields were determined using Eq-1. An increase in temperature
234 decreases the solid residue yields at any pressure for all biomass types, as shown in Figure 5.
235 Residual solids at temperatures up to 150 °C are quite high due to the low ratio of water-soluble
236 components in the lignocellulosic materials. Pressure appears to have an insignificant impact
237 on solubility at these temperatures. The water-soluble portion of the biomass disperses into the
238 water at ~100 °C and hydrolysis starts at temperatures above 150 °C [44]. Each of the 5 biomass
239 feedstocks consists of a different portion of water-soluble compounds at 75 °C. ZB has the
240 highest water-soluble portion (~13-14 wt.%), while the other biomass feedstocks (CR, RW,
241 WW and LG) have only ~2-7 wt.% of water-soluble portions. Conversely, the ratio of
242 hydrolysed compounds at 150 °C is ~7-15 wt.% for CR while it is lower than 5 wt.% for the
243 other biomass feedstocks. Biomass starts to carbonise at temperatures of 180-250 °C [17, 22,
244 25] as the cellulosic and hemicellulosic polymers disintegrates into monomers/oligomers [44].
245

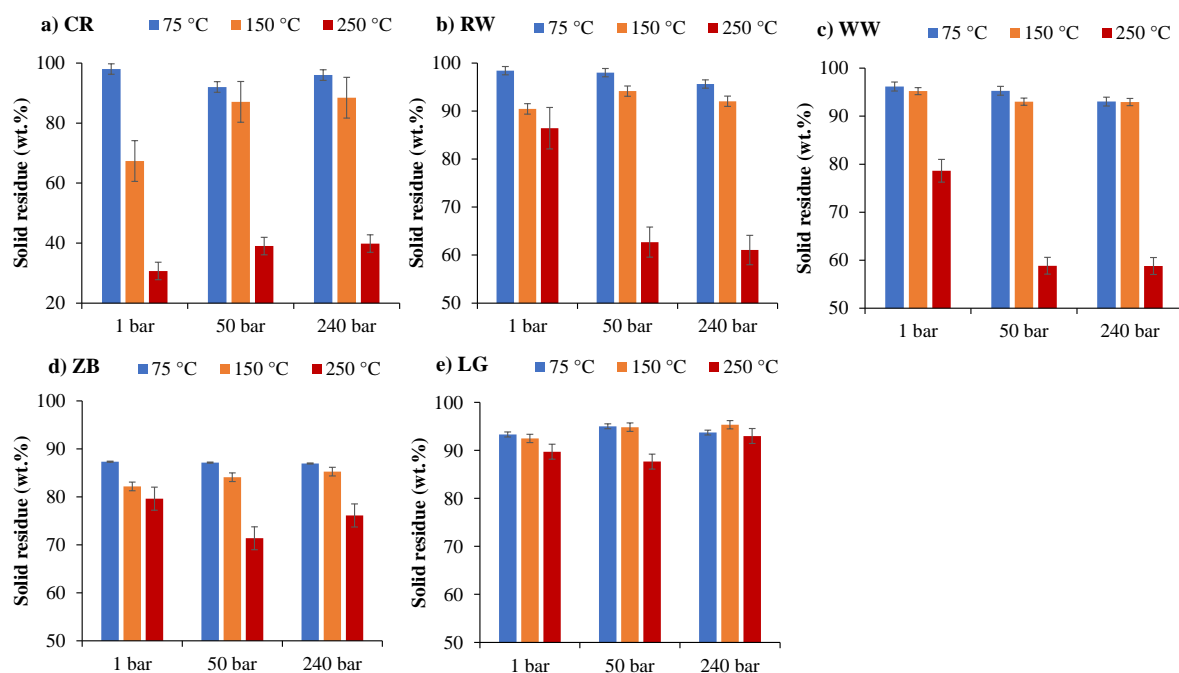


Figure 5. Solid residue (hydrochar) yields of biomasses; a) CR, b) RW, c) WW, and d) ZB and e) LG after the hydrothermal treatment at 75, 150, 250 °C and 1, 50, 240 bar.

CR has the lowest hydrochar yield (39 wt.%) at 250 °C and 50-240 bar and the dW/dt results (in Figure 4) show two clear peaks at ~290 °C and ~330 °C, which represent the higher hemicellulose-cellulose lower cellulose-lignin structures, respectively. The low hydrochar yield is due to the removal of the hemicellulose/cellulose fraction. LG, however, provides the highest hydrochar yield (87-92 wt.%) at relatively severe carbonisation conditions of 250 °C and 50-240 bar due to its low solubility and lack of hemicellulose and cellulose structures. ZB is also resilient to hydrothermal treatment with a high hydrochar yield (71-76 wt.%) at the same conditions. Figure 4 shows LG has a single thermal decomposition peak at ~336 °C. Similar to LG, ZB shows substantial low molecular weight materials evolving at low temperatures (150-225 °C). This could explain why more material solubilised into the water phase for ZB, even at relatively mild conditions. It is possible that the steam explosion breaks down the cell-wall to create lower molecular weight material which is more soluble. The strong peak at ~336 °C in LG and ZB arises from large amounts of cellulose-lignin structures.

Similarly, both RW and WW produce lower hydrochar yields (58-62 wt.%) than LG and ZB. Derivative plots for RW and WW show the presence of shoulder indicating the presence of hemicellulose-cellulose structures. The results provided in Figure 4 and 5 show that the lignocellulosic biomass feedstocks used in this study can be divided into three categories: (i)

268 high hemicellulose-cellulose, lower cellulose-lignin structures, (ii) low hemicellulose-
 269 cellulose, higher cellulose-lignin structures, (iii) cellulose-lignin only structures.

270

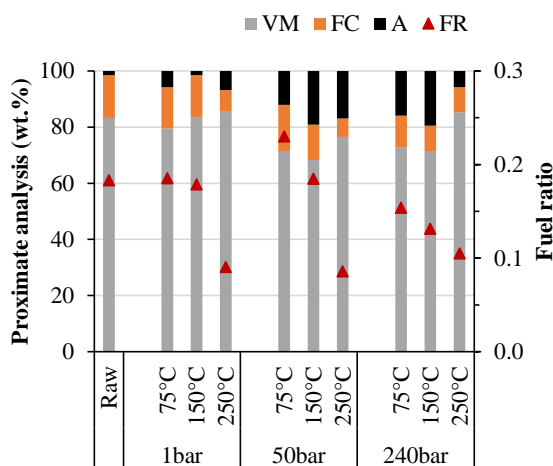
271 **3.3. Thermal analysis of the hydrochars**

272 **3.3.1. High hemicellulose-cellulose, low cellulose-lignin structures (CR)**

273 Figure 6 shows the proximate analysis of hydrochars (or solid residues) produced by the
 274 hydrothermal conversion of CR. The higher temperatures produce a higher ratio of VM and a
 275 lower ratio of FC compared to raw CR, which results in lower fuel ratios at higher temperatures
 276 (Figure 6). Furthermore, the ash content of hydrochars increased consistently particularly at
 277 high pressures.

278

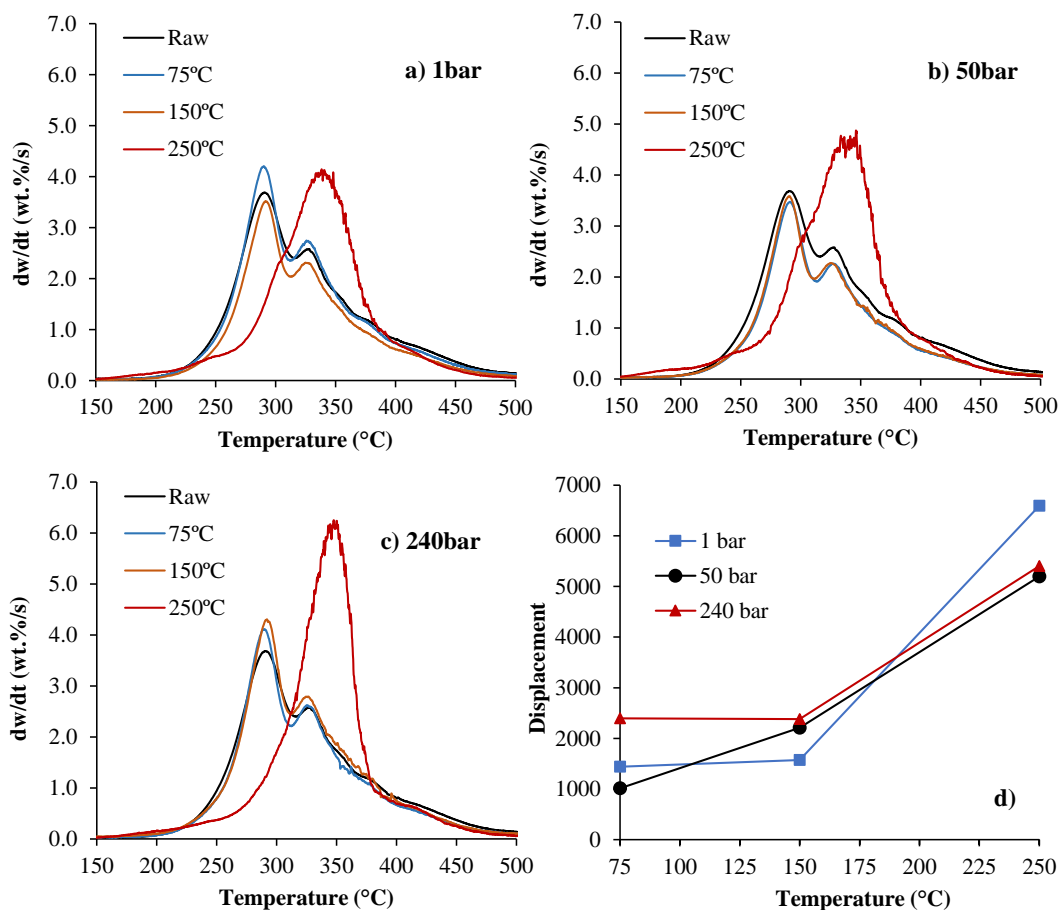
279 Figure 7 presents the derivative weight loss rates of raw and hydrochars produced by the
 280 hydrothermal process of CR and the displacement at the process conditions. The degree of
 281 displacement relates directly to process temperature and pressure. Despite the noise in the
 282 weight loss rates at 250 °C (in Figure 7a-c), there is a remarkable difference between the
 283 thermal decomposition profiles of the hydrochars produced at different conditions.



284

285 **Figure 6.** Proximate analysis (dry basis) of CR and hydrochars produced at the temperatures
 286 of 75-250 °C under the pressure of 1-240 bar. VM – Volatile Matter (db) FC – Fixed Carbon
 287 (db) A – Ash (db) FR – Fuel Ratio (dafb).

288



289

290 **Figure 7.** Weight-loss rates of raw and hydrochars (or solid residues) produced by the
 291 hydrothermal treatment of CR at a) 1 bar, b) 50 bar, c) 240 bar and d) displacement at the
 292 hydrothermal process conditions.

293

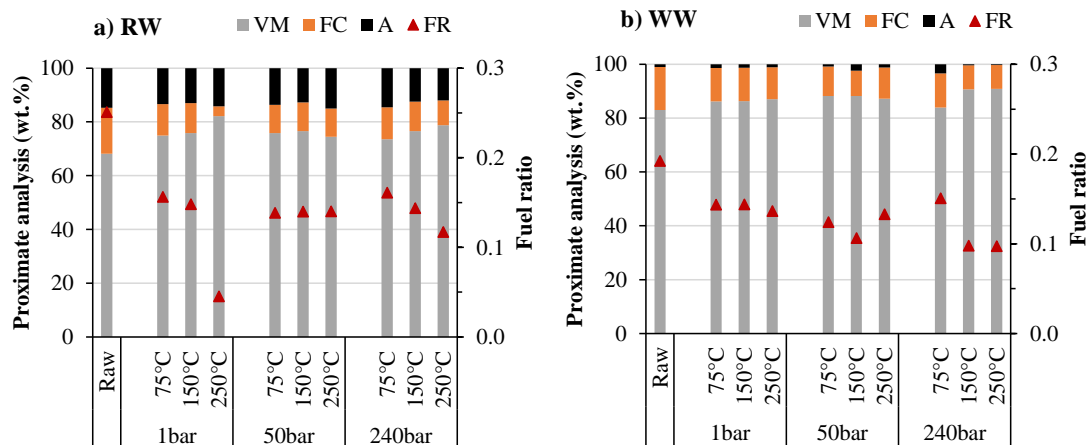
294 The hydrochars produced at lower temperatures (75 $^{\circ}C$ and 150 $^{\circ}C$) provides two
 295 characteristic weight loss rate peaks at ~ 290 $^{\circ}C$ and ~ 330 $^{\circ}C$, which has the similar weight
 296 loss rates compare with the CR feedstock. Additionally, the displacements at these
 297 temperatures do not demonstrate a significant difference as shown in Figure 7d. However,
 298 hydrothermal conversion of CR at 250 $^{\circ}C$ produces a hydrochar with a single thermal
 299 decomposition peak at ~ 340 - 350 $^{\circ}C$ (Figure 7a-c) due to the cellulose-lignin only structures
 300 remaining after the hydrothermal treatment. Hemicellulose appears to have fully solubilized
 301 into the water at a temperature above ~ 160 $^{\circ}C$, effectively under subcritical water conditions
 302 [25]. Since the hemicellulose is an amorphous heteropolysaccharide present as
 303 approximately 20-30 wt.% of the dry weight of most wood species. Hemicellulose forms
 304 hydrogen bonds with cellulose and covalent bonds with lignin (primarily α -benzyl ether
 305 bonds), and ester bonds with hydroxycinnamic acids and acetyl units [45]. The different

306 bonding in hemicellulose compared to cellulose, together with differences in crystallinity
307 and molecular weight mean that the hemicellulose is more easily degraded under
308 hydrothermal treatment, as seen in Figure 7a-c. The first peak disappeared due to a complete
309 degradation of the hemicellulose structures from the CR at 250°C, 1-240 bar. The
310 hydrochars produced at 250 °C, therefore, presents a mixture of low cellulose-high lignin
311 structures, which could result in a higher heating value as lignin has a higher heating value
312 than hemicellulose and cellulose [46]. The weight loss rate was 7.3, 4.5, and 6.0 wt.%/s at
313 250 °C and pressures of 1, 50, and 240 bar. Hydrochars produced at 250 °C, therefore,
314 demonstrate a greater displacement ~5000-7000 as seen in Figure 7d.

315

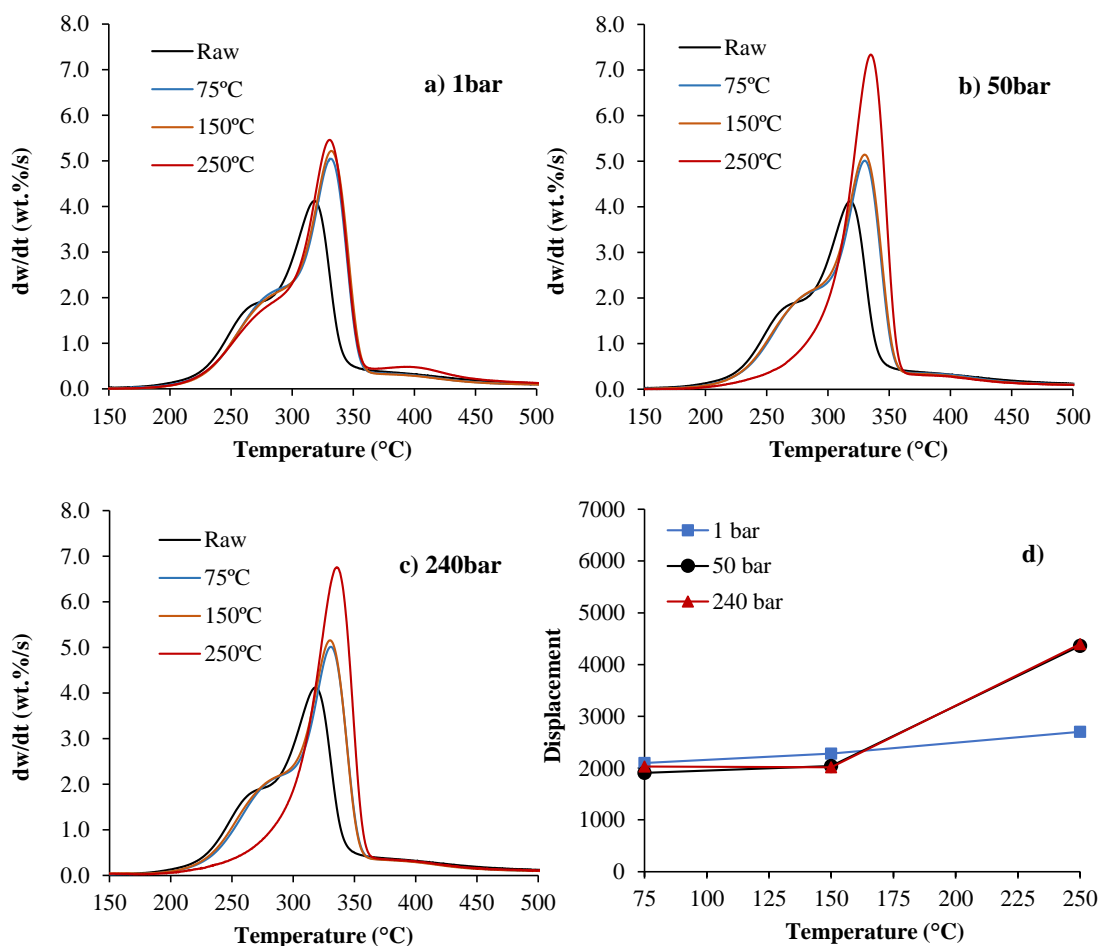
316 ***3.3.2. Lower hemicellulose-cellulose, higher cellulose-lignin structures (RW and WW)***

317 The proximate analysis of hydrochars (or solid residues) produced by the hydrothermal
318 conversion of the biomasses having lower hemicellulose-cellulose and higher cellulose-
319 lignin structures (RW and WW) are presented in Figure 8. Although there is a clear
320 difference in ash content between RW and WW, these two lignocellulosic biomasses show
321 similar levels of thermal decomposition, as a result of their similar hemicellulose, cellulose,
322 and lignin compositions. RW and WW produce a hydrochar with a higher volatile matter
323 and lower fixed carbon contents compared to untreated RW (Figure 8a) and WW (Figure
324 8b). RW has the highest ash content (~15 wt.%) compared with the other biomass
325 feedstocks and the ash content does not change significantly after the hydrothermal
326 treatment. RW ash is predominantly SiO₂ based and insoluble under hydrothermal
327 conditions [47]. Pressure has no effect on the proximate composition of the hydrochars. At
328 250 °C there is an apparent increase in volatile content as a result of the removal of the
329 hemicellulose component, (based on Figure 9a-c) which is not possible at lower
330 temperatures without acid/alkali addition [48]. This increase is only relative to the overall
331 composition of the biochar and caused by the insolubility of the SiO₂ in the RW and the
332 increased solubility of the hemicellulose fraction at 250 °C.



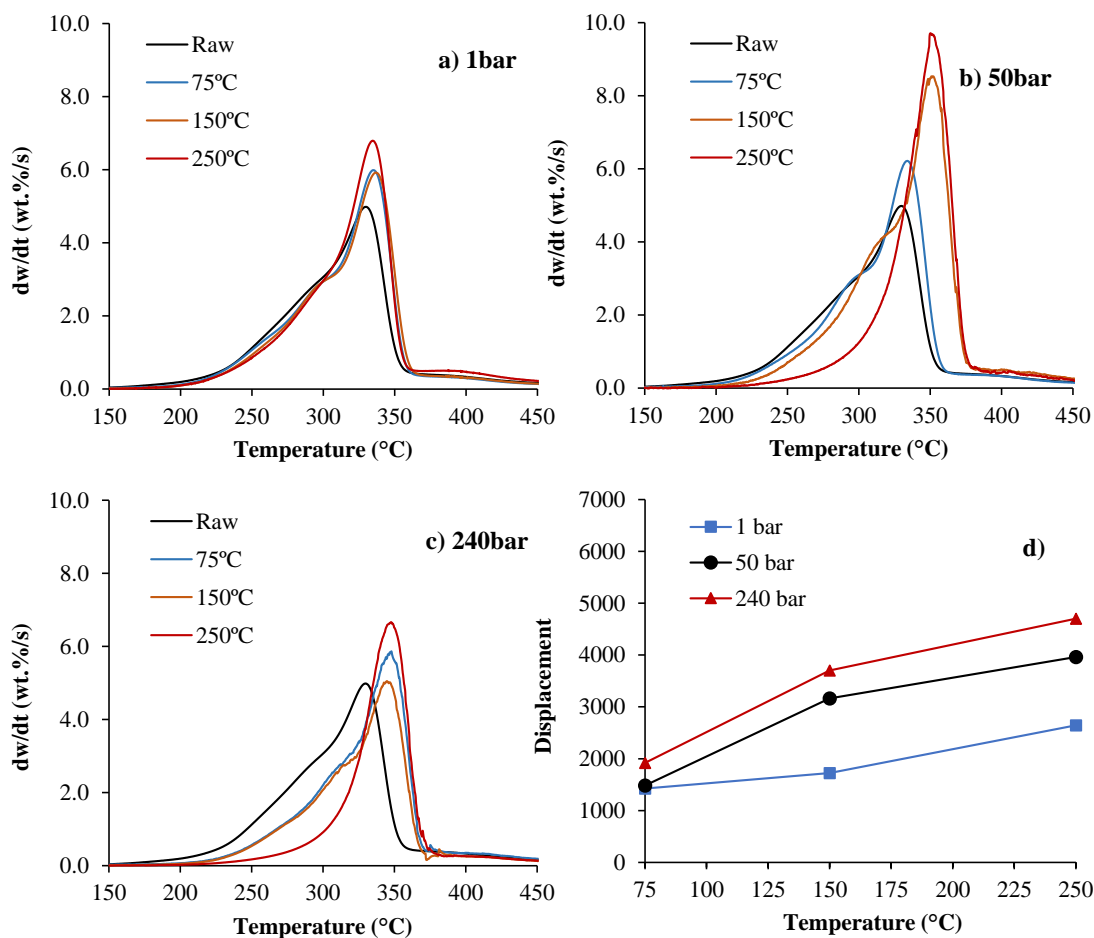
333

334 **Figure 8.** Proximate analysis (dry basis) of a) RW hydrochars and b) WW hydrochars
 335 produced at the temperatures of 75-250°C under the pressure of 1-240 bar. VM – Volatile
 336 Matter (db) FC – Fixed Carbon (db) A – Ash (db) FR – Fuel Ratio (dafb).
 337



338

339 **Figure 9.** Weight-loss rates of raw and hydrochars (or solid residues) produced by the
 340 hydrothermal process of RW at a) 1 bar, b) 50 bar, c) 240 bar and d) displacement at the
 341 hydrothermal process conditions.



342

343 **Figure 10.** Weight-loss rates of raw and hydrochars (or solid residues) produced by the
 344 hydrothermal process of WW at a) 1 bar, b) 50 bar, c) 240 bar and d) displacement at the
 345 hydrothermal process conditions.

346

347 The weight-loss rates and the displacements of RW and WW hydrochars are presented in Figure
 348 9 and Figure 10, respectively. The thermal decomposition of RW hydrochars show a small
 349 detectable shift from 322 $^{\circ}C$ to 333-340 $^{\circ}C$ as seen in Figure 9a-c. The hydrochars produced at
 350 lower temperatures (75 $^{\circ}C$ and 150 $^{\circ}C$) provides similar trends with the raw RW, a strong peak
 351 at ~333 $^{\circ}C$ with a weight loss rate of ~5.2 wt.%/s, (cellulose-lignin) and a shoulder at lower
 352 temperatures of ~304 $^{\circ}C$ (hemicellulose-cellulose) of 2.3 wt.%/s (Figure 9a-c). The
 353 hemicellulose-cellulose levels in RW and WW are much lower than in CR. Therefore, it appears
 354 as a peak in the decomposition of CR (Figure 7a-c) while it is only a shoulder in the
 355 decomposition of RW (Figure 9a-c) and WW (Figure 10a-c). The hemicellulose and cellulose
 356 structures were degraded and solubilised above ~160 $^{\circ}C$ and ~220 $^{\circ}C$, respectively, under
 357 subcritical water conditions [25, 44] due to the catalytic effect of hydroxyl (OH $^{-}$) and
 358 hydronium (H $^{+}$) ions. The shoulder (hemicellulose-cellulose) disappeared at 250 $^{\circ}C$ and 50-

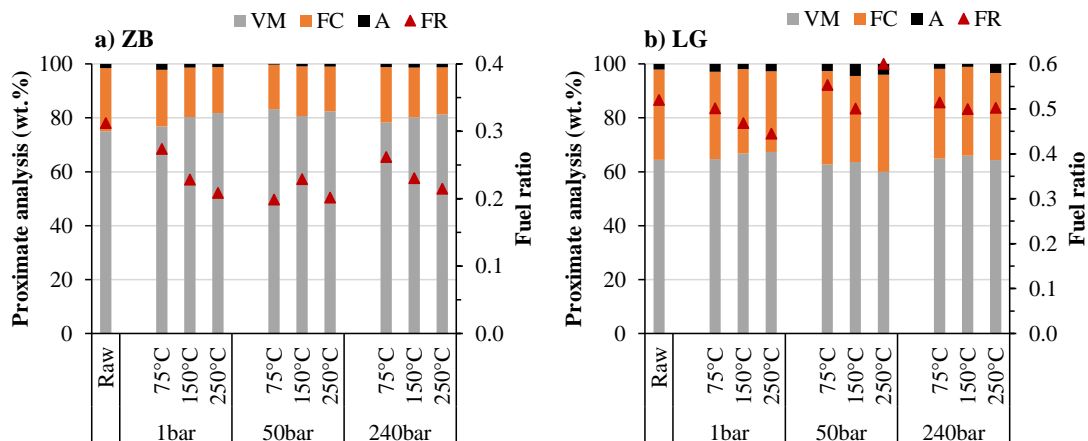
359 240 bar. The displacement (Figure 9d) also demonstrates the similarity with the thermal
 360 decomposition of the solid residues at low temperatures (75 °C and 150 °C) and changes seen
 361 at higher temperatures (250 °C). Neither pressure nor temperature has a significant effect on
 362 the solid residues produced at lower temperatures (75 °C and 150 °C), while a significant
 363 difference was observed for the hydrochars produced at higher temperatures of 250 °C. The
 364 WW hydrochar derivative plots also show a shift to the higher temperature from 333 °C to 340
 365 °C at 1 bar (Figure 10a) and a further shift to ~350 °C at 50 bar and 240 bar (Figure 10b and
 366 10c). The weight-loss rates are ~6.0 wt.%/s at low hydrothermal temperatures (75 °C and 150
 367 °C) and increased to ~6.8 wt.%/s with the temperature increase to 250 °C at 1 bar. The
 368 hydrochars produced at 75 °C and 150 °C indicate the shoulders which indicate the presence of
 369 hemicellulose-cellulose structures. However, the shoulder disappeared at 250 °C, at 50 bar and
 370 240 bar (Figure 10a-c), which is characteristically similar to RW.

371

372 **3.3.3. High cellulose-lignin structures (ZB and LG)**

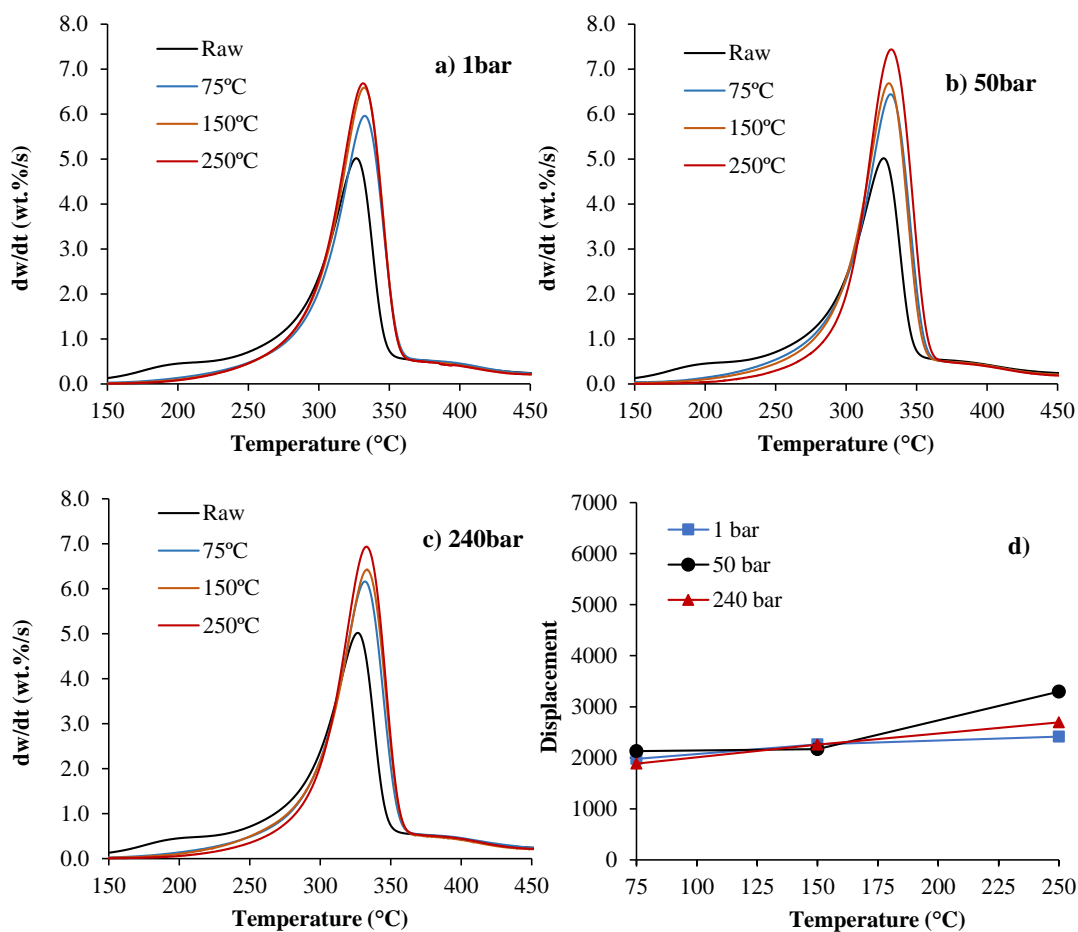
373 Figure 11 shows the proximate analysis of the hydrochars produced by the ZB and LG, which
 374 have a high level of cellulose-lignin structures. These biomasses (ZB and LG) are defined as
 375 having higher FC and lower VM compare to other biomasses, which results in higher fuel ratio
 376 and potentially higher heating value due to higher levels of lignin. The proximate composition
 377 of these two biomass types show insignificant changes during hydrothermal treatment at 75-
 378 250 °C. The small differences could be therefore attributed to the absence of hemicellulose
 379 structures which usually decompose at ~180-200 °C.

380



381

382 **Figure 11.** Proximate analysis (dry basis) of a) ZB hydrochars and b) LG hydrochars
 383 produced at the temperatures of 75-250°C under the pressure of 1-240 bar. VM – Volatile
 384 Matter (db) FC – Fixed Carbon (db) A – Ash (db) FR – Fuel Ratio (dafb).



385

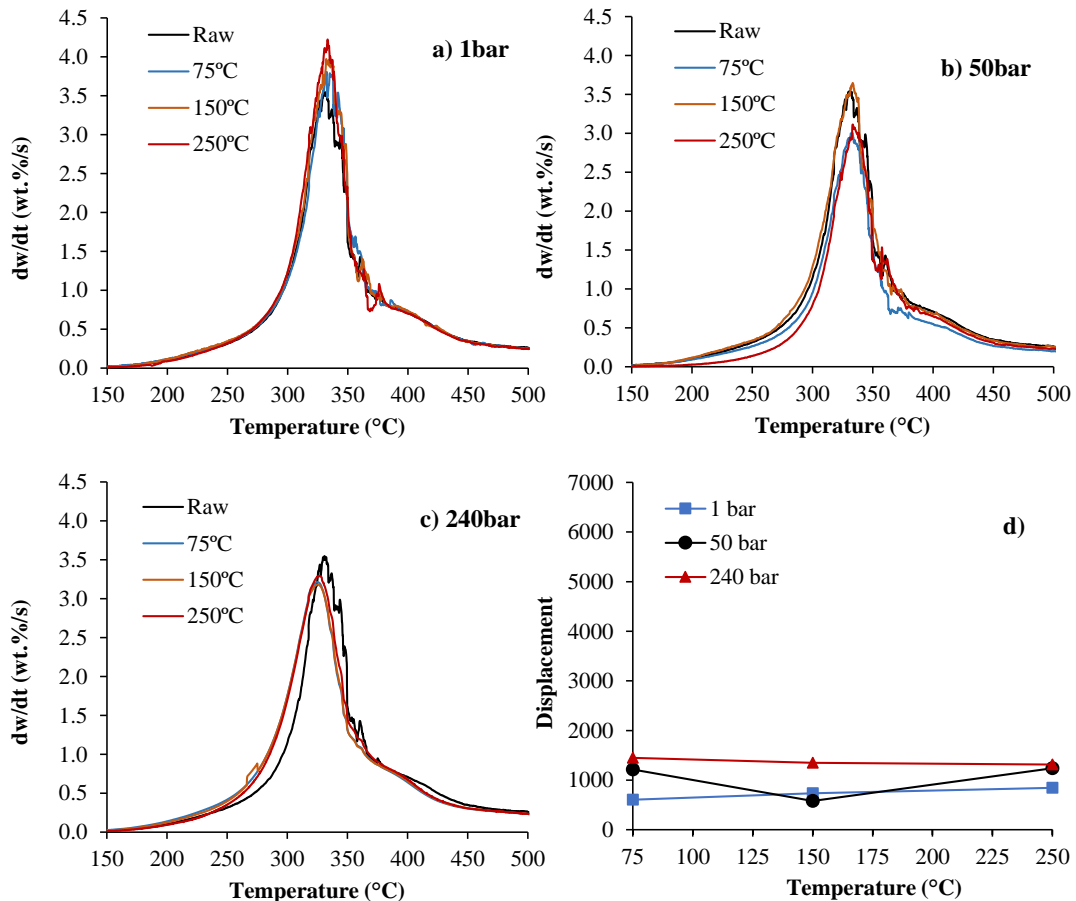
386 **Figure 12.** Weight-loss rates of raw and hydrochars (or solid residues) produced by the
 387 hydrothermal process of ZB at a) 1 bar, b) 50 bar, c) 240 bar and d) displacement at the
 388 hydrothermal process conditions.

389

390 The thermal decomposition of the ZB and LG provides only one peak at ~330 $^{\circ}C$, indicating
 391 that minimal hemicellulose is present. The thermal decomposition of the hydrochars produced
 392 by ZB shows a slight shift to a higher temperature of ~336 $^{\circ}C$ (Figure 12); however, the
 393 hydrochars produced by LG provide similar thermal decomposition profiles compare with the
 394 LG (Figure 13). The slight shift in the ZB hydrochars could be attributed to the decomposition
 395 of cellulose. However, LG hydrochars have cellulosic material and therefore did not provide
 396 any shift in the thermal decomposition, proving that neither pressure nor temperature had a
 397 significant effect on hydrochars generated from biomass with a high lignin content (Figure 13).
 398 The weight-loss rates of ZB hydrochars are ~6-8 wt.%/s when treated at >75 $^{\circ}C$ and do not
 399 show any significant change as pressure changes, as shown in Figure 12. However, the LG
 400 hydrochars show little difference in weight loss rates at any temperature or pressure, as shown
 401 in Figure 13. Unlike CR, WW, RW, ZB and LG both produce minimal displacements (Figure

402 12d and 13d) during hydrothermal conversion, which can be attributed to the high levels of
 403 lignin in ZB and LG. Lignin is an amorphous natural polymer made up of aromatic blocks
 404 which are cross-linked by carbon and ether linkages and considered to be hydrophobic due to
 405 its low solubility in water.

406



407

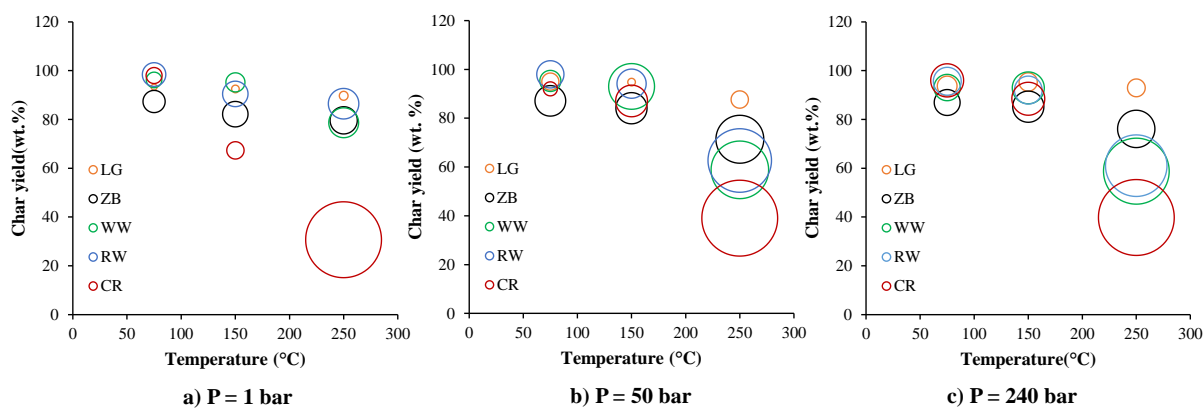
408 **Figure 13.** Weight-loss rates of raw and hydrochars (or solid residues) produced by the
 409 hydrothermal process of LG at a) 1 bar, b) 50 bar, c) 240 bar and d) displacement at the
 410 hydrothermal process conditions.

411

412 3.4. Relationship between Char yield and Displacement

413 Figure 14 shows the relationship between char yield and displacement at the specific
 414 temperature and pressure conditions of hydrothermal treatment. The differences in the
 415 relationship between char yield and displacement of the biomass categories were clearly
 416 demonstrated in Figure 14. Hydrochars produced at lower temperatures (<150 °C) show
 417 relatively small displacements while the hydrochars produced at higher temperature (200 °C)
 418 showed relatively higher displacement.

419



420
421
422
423
424

Figure 14. Relationship between char yield and displacement values under the hydrothermal treatment conditions. The width of bubbles represents the displacement value at each temperature (x axis, 75, 150, 250 °C) and pressure (a) 1 bar, b) 50 bar, c) 240 bar)

425
426
427
428
429
430
431
432
433
434

The highest decomposition and displacement were observed for category (i) biomass feedstocks (CR (red bubbles)) at 250 °C at all pressures. Category (ii) biomass feedstocks (RW (blue bubbles) and WW (green bubbles)) demonstrated the second highest decomposition and displacement, as both hemicellulose and cellulose structures in category (i) and (ii) were successfully degraded under subcritical conditions. The robust lignin structures in category (iii) biomass feedstocks (ZB (black bubbles) and LG (orange bubbles)) resulted in the lowest decomposition and displacement at any temperature and pressure of hydrothermal treatment compared to other two categories. The increase in pressure slightly increases the displacement level of the biomasses at a low temperature (75 °C and 150 °C).

435

4. Conclusions

436
437
438
439
440
441
442
443
444
445
446

This study explored the hydrothermal treatment of biomass in a semi-continuous flow rig. The solid residues at <150 °C and <240 bar did not show any significant structural changes compared with the untreated biomass feedstocks. However, the hydrochars produced at 250 °C and 50 240 bar demonstrates significant structural modifications depending on the biomass type. The first category provided relatively low hydrochar yield (~39 wt.%) due to the degradation of higher hemicellulose-cellulose structures. The second category demonstrated relatively higher hydrochar yields (58-62 wt.%) compared to (i). Category (iii) had the highest hydrochar yields (~73 wt.% for ZB and ~90 wt.% for LG) due to the absence of hemicellulose and generally lower cellulose. The novel displacement analysis method produced a similar trend. Biomass with a higher hemicellulose content produced the highest levels of displacement, with the least displacements resulting from the highest lignin samples. The “displacement”

447 method could thus be a new characterisation technique for the hydrochars to show the
448 quantitative impact of hydrothermal treatment.

449

450 **Acknowledgement**

451 This research was funded and supported by the EPSRC, BBSRC and UK Supergen Bioenergy
452 Hub [Grant number EP/S000771/1].

453

454 **References**

- 455 [1] Lester E, Avila C, Pang CH, Williams O, Perkins J, Gaddipatti S, et al. A proposed biomass
456 char classification system. *Fuel* 2018;232:845-54.
- 457 [2] Shen Y. A review on hydrothermal carbonization of biomass and plastic wastes to energy
458 products. *Biomass and Bioenergy* 2020;134.
- 459 [3] Sharma R, Jasrotia K, Singh N, Ghosh P, srivastava S, Sharma NR, et al. A Comprehensive
460 Review on Hydrothermal Carbonization of Biomass and its Applications. *Chemistry Africa*
461 2019;3(1):1-19.
- 462 [4] Daioglou V, Doelman JC, Wicke B, Faaij A, van Vuuren DP. Integrated assessment of biomass
463 supply and demand in climate change mitigation scenarios. *Global Environmental Change*
464 2019;54:88-101.
- 465 [5] Guo M, Song W. The growing US bioeconomy: Drivers, development and constraints. *New*
466 *biotechnology* 2019;49:48-57.
- 467 [6] Williams O, Newbolt G, Eastwick C, Kingman S, Giddings D, Lormor S, et al. Influence of mill
468 type on densified biomass comminution. *Applied Energy* 2016;182:219-31.
- 469 [7] Williams O, Eastwick C, Kingman S, Giddings D, Lormor S, Lester E. Investigation into the
470 applicability of Bond Work Index (BWI) and Hardgrove Grindability Index (HGI) tests for
471 several biomasses compared to Colombian La Loma coal. *Fuel* 2015;158:379-87.
- 472 [8] Vassilev SV, Vassileva CG, Vassilev VS. Advantages and disadvantages of composition and
473 properties of biomass in comparison with coal: An overview. *Fuel* 2015;158:330-50.
- 474 [9] Isikgor FH, Becer CR. Lignocellulosic biomass: a sustainable platform for the production of
475 bio-based chemicals and polymers. *Polymer Chemistry* 2015;6(25):4497-559.
- 476 [10] Antero RVP, Alves ACF, de Oliveira SB, Ojala SA, Brum SS. Challenges and alternatives for
477 the adequacy of hydrothermal carbonization of lignocellulosic biomass in cleaner production
478 systems: A review. *Journal of Cleaner Production* 2020;252.
- 479 [11] Wang S, Dai G, Yang H, Luo Z. Lignocellulosic biomass pyrolysis mechanism: a state-of-the-
480 art review. *Progress in Energy and Combustion Science* 2017;62:33-86.
- 481 [12] Ruiz HA, Rodríguez-Jasso RM, Fernandes BD, Vicente AA, Teixeira JA. Hydrothermal
482 processing, as an alternative for upgrading agriculture residues and marine biomass according
483 to the biorefinery concept: a review. *Renewable and Sustainable Energy Reviews* 2013;21:35-
484 51.
- 485 [13] Pedersen TH, Grigoras I, Hoffmann J, Toor SS, Daraban IM, Jensen CU, et al. Continuous
486 hydrothermal co-liquefaction of aspen wood and glycerol with water phase recirculation.
487 *Applied energy* 2016;162:1034-41.
- 488 [14] Kumar M, Oyedun AO, Kumar A. A review on the current status of various hydrothermal
489 technologies on biomass feedstock. *Renewable and Sustainable Energy Reviews* 2018;81:1742-
490 70.
- 491 [15] Cherad R, Onwudili J, Biller P, Williams P, Ross A. Hydrogen production from the catalytic
492 supercritical water gasification of process water generated from hydrothermal liquefaction of
493 microalgae. *Fuel* 2016;166:24-8.

- 494 [16] Abdoulmoumine N, Adhikari S, Kulkarni A, Chattanathan S. A review on biomass gasification
495 syngas cleanup. *Applied Energy* 2015;155:294-307.
- 496 [17] Elliott DC, Biller P, Ross AB, Schmidt AJ, Jones SB. Hydrothermal liquefaction of biomass:
497 developments from batch to continuous process. *Bioresource technology* 2015;178:147-56.
- 498 [18] Dimitriadis A, Bezergianni S. Hydrothermal liquefaction of various biomass and waste
499 feedstocks for biocrude production: A state of the art review. *Renewable and Sustainable Energy*
500 *Reviews* 2017;68:113-25.
- 501 [19] Şimşek EH, Güleç F, Akçadağ FS. Understanding the liquefaction mechanism of Beypazarı
502 lignite in tetralin with ultraviolet irradiation using discrete time models. *Fuel Processing*
503 *Technology* 2020;198:106227.
- 504 [20] Güleç F, Özdemir GDT. Investigation of drying characteristics of Cherry Laurel (*Laurocerasus*
505 *officinalis* Roemer) fruits. *Akademik ziraat dergisi* 2017;6(1):73-80.
- 506 [21] Heidari M, Norouzi O, Salaudeen S, Acharya B, Dutta A. Prediction of Hydrothermal
507 Carbonization with Respect to the Biomass Components and Severity Factor. *Energy & Fuels*
508 2019;33(10):9916-24.
- 509 [22] Arellano O, Flores M, Guerra J, Hidalgo A, Rojas D, Strubinger A. Hydrothermal
510 carbonization (HTC) of corncob and characterization of the obtained hydrochar. *Chemical*
511 *Engineering* 2016;50.
- 512 [23] Wei L, Sevilla M, Fuertes AB, Mokaya R, Yushin G. Hydrothermal carbonization of abundant
513 renewable natural organic chemicals for high - performance supercapacitor electrodes.
514 *Advanced Energy Materials* 2011;1(3):356-61.
- 515 [24] Álvarez-Murillo A, Sabio E, Ledesma B, Román S, González-García C. Generation of biofuel
516 from hydrothermal carbonization of cellulose. *Kinetics modelling. Energy* 2016;94:600-8.
- 517 [25] Heidari M, Dutta A, Acharya B, Mahmud S. A review of the current knowledge and challenges
518 of hydrothermal carbonization for biomass conversion. *Journal of the Energy Institute*
519 2019;92(6):1779-99.
- 520 [26] Kambo HS, Dutta A. Strength, storage, and combustion characteristics of densified
521 lignocellulosic biomass produced via torrefaction and hydrothermal carbonization. *Applied*
522 *Energy* 2014;135:182-91.
- 523 [27] Subedi R, Kammann C, Pelissetti S, Sacco D, Grignani C, Monaco S. Recycling of organic
524 residues for agriculture: from waste management to ecosystem services. 15th International
525 Conference RAMIRAN. 2013.
- 526 [28] Guangzhi Y, Jinyu Y, Yuhua Y, Zhihong T, DengGuang Y, Junhe Y. Preparation and CO₂
527 adsorption properties of porous carbon from camphor leaves by hydrothermal carbonization and
528 sequential potassium hydroxide activation. *RSC advances* 2017;7(7):4152-60.
- 529 [29] Liu Z, Zhang F, Hoekman SK, Liu T, Gai C, Peng N. Homogeneously dispersed zerovalent iron
530 nanoparticles supported on hydrochar-derived porous carbon: simple, in situ synthesis and use
531 for dechlorination of PCBs. *ACS Sustainable Chemistry & Engineering* 2016;4(6):3261-7.
- 532 [30] Fan F, Xing X, Shi S, Zhang X, Zhang X, Li Y, et al. Combustion characteristic and kinetics
533 analysis of hydrochars. *Transactions of the Chinese Society of Agricultural Engineering*
534 2016;32(15):219-24.
- 535 [31] Hao W, Björkman E, Lilliestråle M, Hedin N. Activated carbons for water treatment prepared
536 by phosphoric acid activation of hydrothermally treated beer waste. *Industrial & Engineering*
537 *Chemistry Research* 2014;53(40):15389-97.
- 538 [32] Titirici M-M, Antonietti M, Baccile N. Hydrothermal carbon from biomass: a comparison of
539 the local structure from poly- to monosaccharides and pentoses/hexoses. *Green Chemistry*
540 2008;10(11):1204-12.
- 541 [33] Lester E, Gong M, Thompson A. A method for source apportionment in biomass/coal blends
542 using thermogravimetric analysis. *Journal of analytical and applied pyrolysis* 2007;80(1):111-
543 7.
- 544 [34] Kostas ET, Williams OS, Duran-Jimenez G, Tapper AJ, Cooper M, Meehan R, et al. Microwave
545 pyrolysis of *Laminaria digitata* to produce unique seaweed-derived bio-oils. *Biomass and*
546 *Bioenergy* 2019;125:41-9.

- 547 [35] Kostas ET, White DA, Cook DJ. Development of a bio-refinery process for the production of
548 speciality chemical, biofuel and bioactive compounds from *Laminaria digitata*. *Algal research*
549 2017;28:211-9.
- 550 [36] Paczkowski S, Sauer C, Anetzberger A, Paczkowska M, Russ M, Wöhler M, et al. Feedstock
551 particle size distribution and water content dynamic in a pellet mill production process and
552 comparative sieving performance of horizontal 3.15-mm mesh and 3.15-mm hole sieves.
553 *Biomass Conversion and Biorefinery* 2019:1-12.
- 554 [37] EN-ISO-17827-2. Solid biofuels - determination of particle size distribution for uncompressed
555 fuels: Part 2: Vibrating screen method using sieves with aperture of 3,15 mm and below (17827-
556 2:2016-10). DIN Deutsches Institut für Normung; 2016.
- 557 [38] Koechermann J, Goersch K, Wirth B, Muehlenberg J, Klemm M. Hydrothermal carbonization:
558 Temperature influence on hydrochar and aqueous phase composition during process water
559 recirculation. *Journal of Environmental Chemical Engineering* 2018;6(4):5481-7.
- 560 [39] Ninduangdee P, Kuprianov VI, Cha EY, Kaewrath R, Youngyuen P, Atthawethworawuth W.
561 Thermogravimetric studies of oil palm empty fruit bunch and palm kernel shell: TG/DTG
562 analysis and modeling. *Energy Procedia* 2015;79:453-8.
- 563 [40] Pang CH, Gaddipatti S, Tucker G, Lester E, Wu T. Relationship between thermal behaviour of
564 lignocellulosic components and properties of biomass. *Bioresource technology* 2014;172:312-
565 20.
- 566 [41] Gollakota AR, Reddy M, Subramanyam MD, Kishore N. A review on the upgradation
567 techniques of pyrolysis oil. *Renewable and Sustainable Energy Reviews* 2016;58:1543-68.
- 568 [42] Carrier M, Auret L, Bridgwater A, Knoetze JH. Using apparent activation energy as a reactivity
569 criterion for biomass pyrolysis. *Energy & Fuels* 2016;30(10):7834-41.
- 570 [43] Yang H, Yan R, Chen H, Lee DH, Zheng C. Characteristics of hemicellulose, cellulose and
571 lignin pyrolysis. *Fuel* 2007;86(12-13):1781-8.
- 572 [44] Tekin K, Karagöz S, Bektaş S. A review of hydrothermal biomass processing. *Renewable and*
573 *sustainable Energy reviews* 2014;40:673-87.
- 574 [45] Ren J, Sun R. Hemicelluloses. *Cereal straw as a resource for sustainable biomaterials and*
575 *biofuels* Amsterdam: Elsevier 2010:73-130.
- 576 [46] Vassilev SV, Baxter D, Andersen LK, Vassileva CG, Morgan TJ. An overview of the organic
577 and inorganic phase composition of biomass. *Fuel* 2012;94:1-33.
- 578 [47] Ludueña LN, Fasce DP, Alvarez VA, Stefani PM. Nanocellulose from rice husk following
579 alkaline treatment to remove silica. *BioResources* 2011;6(2):1440-53.
- 580 [48] Barana D, Salanti A, Orlandi M, Ali DS, Zoia L. Biorefinery process for the simultaneous
581 recovery of lignin, hemicelluloses, cellulose nanocrystals and silica from rice husk and *Arundo*
582 *donax*. *Industrial Crops and Products* 2016;86:31-9.
- 583